

Notes

Observed Instability of Bound Pybox Ligands towards Acetate Counterions

Abul B. Kazi,[†] Gavin D. Jones,[‡] and David A. Vicic^{*,‡}

Department of Chemistry and Biochemistry, University of Arkansas, Fayetteville, Arkansas 72701, and Department of Chemistry and Physics, University of Arkansas at Pine Bluff, 1200 North University Drive, Pine Bluff, Arkansas 71601

Received September 1, 2005

Summary: Reaction of Pd(OAc)₂ with bis(oxazolinyl)-pyridine (pybox) ligands led cleanly to products that contained a ring-opened oxazoline ring. The transformations were formally the result of the attack of bound pybox ligands by acetate counterions, leading to acetate incorporation into the ring-opened products.

Introduction

The tridentate pybox ligand is one of the most successful ligands employed in asymmetric catalysis.^{1–24}

* To whom correspondence should be addressed. E-mail: dvicic@uark.edu.

[†] University of Arkansas at Pine Bluff.

[‡] University of Arkansas.

(1) Aspinall, H. C.; Greeves, N. *J. Organomet. Chem.* **2002**, *647*, 151–157.

(2) Nishiyama, H. *Enantiomer* **1999**, *4*, 569–574.

(3) Doyle, M. P.; Protopopova, M. N. *Tetrahedron* **1998**, *54*, 7919–7946.

(4) Nishiyama, H. *Adv. Catal. Processes* **1997**, *2*, 153–188.

(5) Nishiyama, H.; Itoh, K. *Yuki Gosei Kagaku Kyokaiishi* **1995**, *53*, 500–508.

(6) Johnson, J. S.; Evans, D. A. *Acc. Chem. Res.* **2000**, *33*, 325–335.

(7) Evans, D. A.; Fandrick, K. R.; Song, H.-J. *J. Am. Chem. Soc.* **2005**, *127*, 8942–8943.

(8) Suga, H.; Inoue, K.; Inoue, S.; Kakehi, A.; Shiro, M. *J. Org. Chem.* **2005**, *70*, 47–56.

(9) Evans, D. A.; Scheidt, K. A.; Fandrick, K. R.; Lam, H. W.; Wu, J. *J. Am. Chem. Soc.* **2003**, *125*, 10780–10781.

(10) Suga, H.; Inoue, K.; Inoue, S.; Kakehi, A. *J. Am. Chem. Soc.* **2002**, *124*, 14836–14837.

(11) Esteruelas, M. A.; Lopez, A. M.; Mendez, L.; Olivan, M.; Onate, E. *New J. Chem.* **2002**, *26*, 1542–1544.

(12) Iwasa, S.; Maeda, H.; Nishiyama, K.; Tsushima, S.; Tsukamoto, Y.; Nishiyama, H. *Tetrahedron* **2002**, *58*, 8281–8287.

(13) Iwasa, S.; Tsushima, S.; Shimada, T.; Nishiyama, H. *Tetrahedron* **2002**, *58*, 227–232.

(14) Evans, D. A.; Sweeney, Z. K.; Rovis, T.; Tedrow, J. S. *J. Am. Chem. Soc.* **2001**, *123*, 12095–12096.

(15) Zhao, C.-X.; Duffey, M. O.; Taylor, S. J.; Morken, J. P. *Org. Lett.* **2001**, *3*, 1829–1831.

(16) Schaus, S. E.; Jacobsen, E. N. *Org. Lett.* **2000**, *2*, 1001–1004.

(17) Evans, D. A.; Barnes, D. M.; Johnson, J. S.; Lectka, T.; von Matt, P.; Miller, S. J.; Murry, J. A.; Norcross, R. D.; Shaughnessy, E. A.; Campos, K. R. *J. Am. Chem. Soc.* **1999**, *121*, 7582–7594.

(18) Evans, D. A.; Murry, J. A.; Kozlowski, M. C. *J. Am. Chem. Soc.* **1996**, *118*, 5814–5815.

(19) DattaGupta, A.; Singh, V. K. *Tetrahedron Lett.* **1996**, *37*, 2633–2636.

(20) Nishiyama, H.; Itoh, Y.; Matsumoto, H.; Park, S.-B.; Itoh, K. *J. Am. Chem. Soc.* **1994**, *116*, 2223–2224.

(21) Nishiyama, H.; Kondo, M.; Nakamura, T.; Itoh, K. *Organometallics* **1991**, *10*, 500–508.

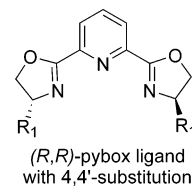
(22) Arp, F. O.; Fu, G. C. *J. Am. Chem. Soc.* **2005**, *127*, 10482–10483.

(23) Fischer, C.; Fu, G. C. *J. Am. Chem. Soc.* **2005**, *127*, 4594–4595.

The tridentate chelation of the nitrogen atoms imparts stability to the resulting metal complexes, and the ability to substitute at the 3- and 4-positions of the oxazoline ring affords the opportunity to tune the steric and stereo environment near the metal center. Despite the large number of metals which have been used successfully with pybox, there have been surprisingly only four reports of catalysis with palladium pybox complexes, and the only structurally characterized complexes contained the noncoordinating BF₄ counterion.^{25–28} Our laboratory has been actively exploring the use of nickel compounds containing tridentate nitrogen donor ligands for alkyl–alkyl cross-coupling catalysis.^{29,30} In hopes of preparing new palladium analogues to compare with the nickel catalysts, we explored a number of ways to attach a pybox ligand to readily available palladium precursors. Here, we report an attempt to prepare a palladium pybox acetate complex and a ring-opening reaction of the oxazoline ring that ensues with the more reactive acetate counterion.

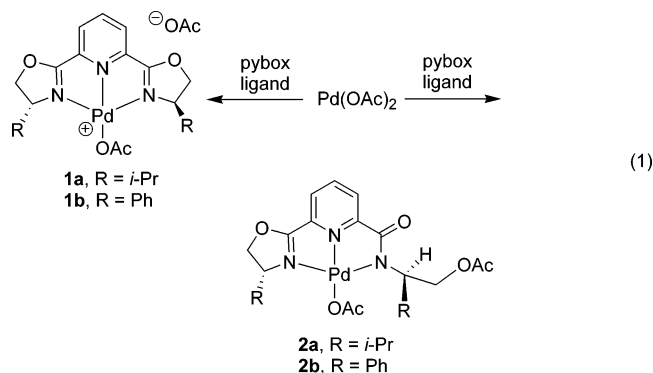
Results and Discussion

Initially we set out to prepare the two pybox derivatives **1** containing differing substitution at the 4- and 4'-positions of the oxazoline ring.



It was found that reaction of Pd(OAc)₂ with **1** equiv of the pybox ligand in THF for 3 h at 70 °C did not lead to the expected acetates **1** but instead led to the ring-opened derivatives **2** (eq 1). The ¹H NMR spectra of **2** clearly confirm the loss of C₂ symmetry in the bound ligands and also show the presence of two acetate groups in magnetically different environments. The new ring-opened products were insoluble in benzene, which aided in the purification from unreacted ligand and other

(24) Desimoni, G.; Faita, G.; Quadrelli, P. *Chem. Rev.* **2003**, *103*, 3119–3154.



unidentified products. This ring-opening reaction occurred for both of the pybox ligands examined in identical isolated yields of 40%.

X-ray-quality crystals were grown from slow diffusion of pentane into saturated THF solutions of **2a**, and the ORTEP diagram of the refined structure is shown in Figure 1. The structure was solved by anomalous dispersion methods in the $P2_1$ space group; however, the PLATON program³¹ suggests a higher symmetry in the orthorhombic setting. All attempts to solve the structure in the suggested $P2_12_12_1$ space group of higher symmetry were unsuccessful. Compound **2a** crystallized as stacked dimers (Figure 2) in a head-to-tail arrangement that maximizes overlap of the aromatic pyridine rings. The intermolecular distance between C9 and the palladium atom of its stacked pair is 3.42 Å.

Compound **2b** does not crystallize in the orthorhombic setting ($P2_12_12_1$), and the ORTEP diagram of **2b** is shown in Figure 3. The packing diagram of **2b** reveals repeating units of a closely packed arrangement of three independent molecules (Figure 4). The most notable feature of the packing arrangement for **2b** is the long hydrogen bond of 2.88 Å between H13 and a neighboring palladium atom (Figures 4 and 5). These nonbonding aryl hydrogen interactions to palladium appear to be common, as over 200 entries were found in a search in the Cambridge Structural Database.³² The cavity that is left by this hydrogen bonding is then occupied by the phenyl ring of a pybox ligand of a third molecule (Figure 4).

We suggest two plausible mechanisms to account for the ring opening of the oxazoline fragment (Scheme 1). Mechanism A involves attack of the acetate at the 3-position of the ring in an S_N2 -like fashion to afford **2**. Alternatively, the acetate can attack at the imine carbon of the ring followed by COMe transfer, as outlined in mechanism B. The openings to provide **2** are highly reminiscent of the transformation observed by Chevallier and co-workers, who found that heating oxazolines

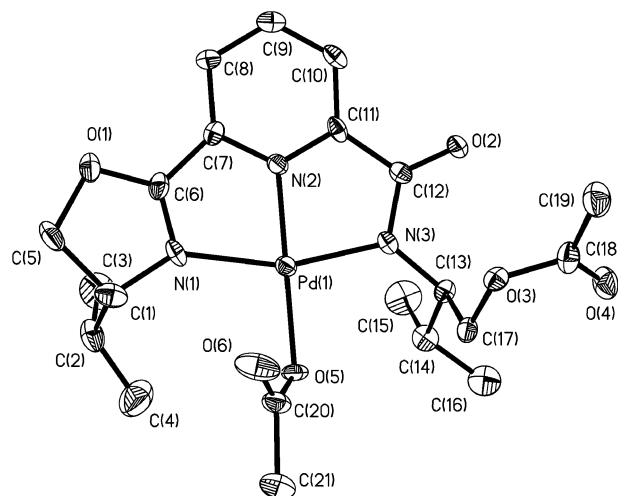


Figure 1. ORTEP diagram of **2a**. Ellipsoids are shown at the 30% level. Hydrogen atoms are omitted for clarity. Selected bond lengths (Å): Pd(1)–N(2), 1.948(6); Pd(1)–O(5), 2.021(5); Pd(1)–N(3), 2.028(6); Pd(1)–N(1), 2.092(6); O(2)–C(12), 1.243(8); O(1)–C(6), 1.326(9); N(3)–C(13), 1.470(10). Selected bond angles (deg): N(2)–Pd(1)–O(5), 177.3(3); N(2)–Pd(1)–N(3), 81.5(3); O(5)–Pd(1)–N(3), 98.9(2); N(2)–Pd(1)–N(1), 79.0(3); O(5)–Pd(1)–N(1), 100.7(2); N(3)–Pd(1)–N(1), 160.4(3); O(2)–C(12)–N(3), 125.8(7); O(2)–C(12)–C(11), 121.7(7).

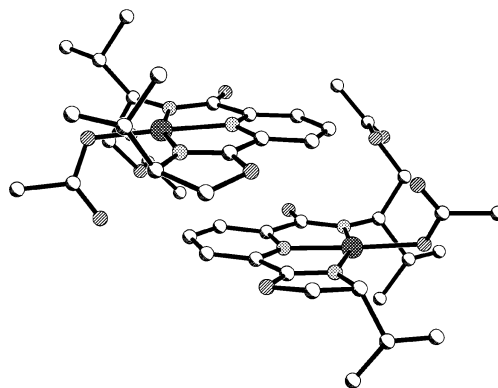
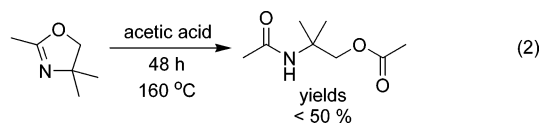


Figure 2. Stacking diagram of **2a**. Hydrogen atoms are omitted for clarity.

in acetic acid under forcing conditions provided the corresponding acetate adducts (eq 2).³³ The lower tem-



peratures needed for the palladium-bound pybox ligands suggest a strong Lewis acid effect in the ring-opening reactions.

Conclusion

Attempts to prepare an intact (pybox)Pd(OAc)₂ complex were unsuccessful. However, the inorganic products of the reaction were successfully isolated and structurally characterized. The X-ray structures reveal that the bound pybox ligands are susceptible to formal attack

(25) Leung, W.-H.; Mak, W.-L.; Chan, E. Y. Y.; Lam, T. C. H.; Lee, W.-S.; Kwong, H.-L.; Yeung, L.-L. *Synlett* **2002**, 1688–1690.

(26) Jiang, M.; Dalgarno, S.; Kilner, C. A.; Halcrow, M. A.; Kee, T. P. *Polyhedron* **2001**, *20*, 2151–2162.

(27) Nesper, R.; Pregosin, P.; Puentener, K.; Woerle, M.; Albinati, A. *J. Organomet. Chem.* **1996**, *507*, 85–101.

(28) Nesper, R.; Pregosin, P. S.; Puentener, K.; Woerle, M. *Helv. Chim. Acta* **1993**, *76*, 2239–2249.

(29) Anderson, T. J.; Jones, G. D.; Vivic, D. A. *J. Am. Chem. Soc.* **2004**, *126*, 8100–8101, 11113 (addition and correction).

(30) Jones, G. D.; McFarland, C.; Anderson, T. J.; Vivic, D. A. *Chem. Commun.* **2005**, 4211–4213.

(31) Spek, A. L. *J. Appl. Crystallogr.* **2003**, *36*, 7–13.

(32) The search was performed using ConQuest software with a defined intermolecular Pd···H–Ar distance between 2.0 and 3.0 Å.

(33) Chevallier, P.; Soutif, J.-C.; Brosse, J.-C.; Rincon-Guerrero, A. *Eur. Polym. J.* **1998**, *34*, 767–778.

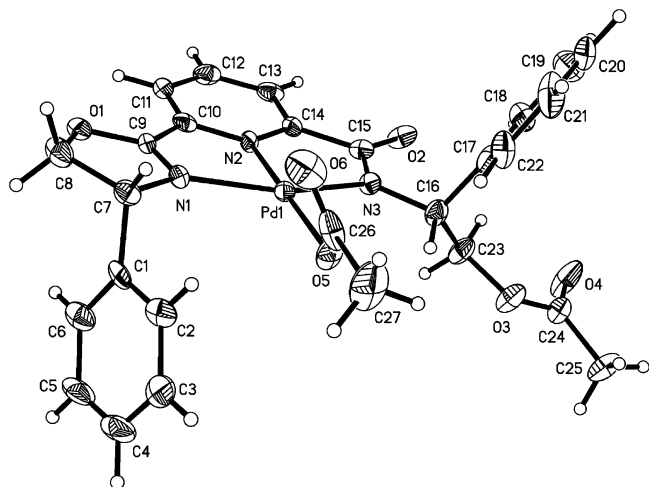


Figure 3. ORTEP diagram of **2b**. Ellipsoids are shown at the 30% level. Selected bond lengths (Å): Pd(1)–N(2), 1.960(7); Pd(1)–N(3), 2.015(7); Pd(1)–O(5), 2.020(8); Pd(1)–N(1), 2.089(8); O(2)–C(15), 1.233(10); N(3)–C(15), 1.340(11). Selected bond angles (deg): N(2)–Pd(1)–N(3), 80.7(3); N(2)–Pd(1)–O(5), 174.2(3); N(3)–Pd(1)–O(5), 95.2(3); N(2)–Pd(1)–N(1), 79.3(4); N(3)–Pd(1)–N(1), 159.9(3); O(5)–Pd(1)–N(1), 104.9(3); O(2)–C(15)–N(3), 128.2(9); O(2)–C(15)–C(14), 118.7(8).

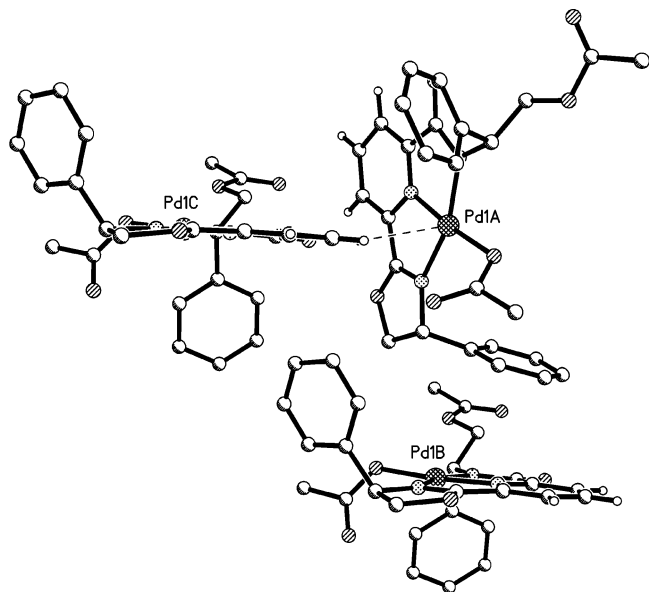


Figure 4. Partial packing diagram of **2b** showing the trinuclear repeating units.

by acetate counterions to afford new ring-opened palladium amido complexes. On the basis of the results presented here, the susceptibility to acetates should be carefully considered when using the pybox ligand in metal-mediated catalysis.

Experimental Section

General Considerations. All manipulations were performed using standard Schlenk techniques or in a nitrogen-filled glovebox, unless otherwise noted. Solvents were distilled from appropriate drying agents before use. All reagents were used as received from commercial vendors unless otherwise noted. Elemental analyses were performed by Desert Analytics. ^1H NMR spectra were recorded at ambient temperature on a Bruker Avance 300 MHz spectrometer and referenced to

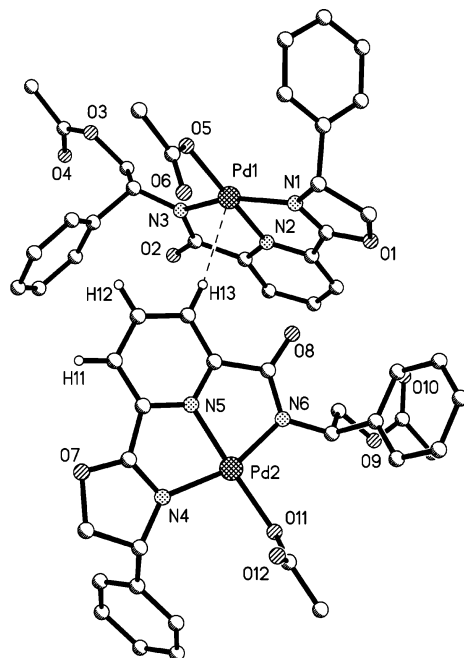
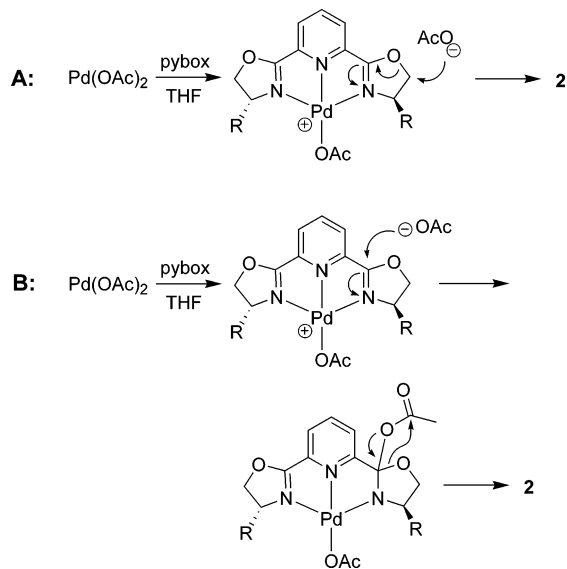


Figure 5. Close-up view of the intermolecular contact between the pyridyl hydrogen and a neighboring palladium atom in **2b**.

Scheme 1. Plausible Mechanisms for the Formation of **2**



residual proton solvent peaks. A Rigaku MSC Mercury/AFC8 diffractometer was used for X-ray structural determinations.

Synthesis of **2a.** (*R,R*)-2,6-Bis(4-isopropoyl-2-oxazolin-2-yl)pyridine (671 mg, 2.23 mmol) and $\text{Pd}(\text{OAc})_2$ (500 mg, 2.23 mmol) were suspended in 100 mL of THF and heated at 70 °C for 3 h. The solvent was then removed under vacuum, and the residue was washed with benzene, leaving **2a** as a greenish brown solid. Crude yield: 470 mg, 40%. Yellow crystals were obtained by recrystallization with THF and pentane. ^1H NMR (CDCl_3): δ 8.13 (t, $J = 7.9$ Hz, 1H), 7.91 (dd, $J = 8.1, 0.9$ Hz, 1H), 7.62 (dd, $J = 7.73, 0.94$ Hz, 1H), 4.81–4.67 (m, 2H), 4.56–4.43 (m, 2H), 4.03–3.71 (m, 2H), 2.17–2.06 (m, 1H), 2.03 (s, 3H), 2.00 (s, 3H), 1.86–1.77 (m, 1H), 1.08 (d, $J = 6.97$ Hz, 3H), 1.00 (d, $J = 6.70$ Hz, 3H), 0.95 (dd, $J = 6.97$ Hz, 1.95 Hz, 6H). $^{13}\text{C}\{^1\text{H}\}$ NMR (CDCl_3 , 22 °C, 75 MHz): δ 178.3, 171.5, 169.7, 167.2, 156.4, 141.8, 140.9, 127.5, 124.1, 73.4, 68.6, 66.1, 60.2, 30.1, 29.6, 23.2, 21.4, 20.9, 20.2, 18.8, 15.4. Anal. Calcd for $\text{C}_{21}\text{H}_{29}\text{N}_3\text{O}_6$: C, 47.91 (47.96); H, 5.25 (5.56).

Synthesis of 2b. (*R,R*)-2,6-Bis(4-phenyl-2-oxazolin-2-yl)pyridine (329 mg, 0.89 mmol) and Pd(OAc)₂ (200 mg, 0.89 mmol) were suspended in 50 mL of THF and heated at 70 °C for 3 h. The solvent was then removed under vacuum, and the residue was washed with benzene, leaving **2b** as a greenish brown solid. Crude yield: 210 mg, 40%. Yellow crystals were obtained by recrystallization with THF and pentane. ¹H NMR (CDCl₃): δ 8.10 (t, *J* = 7.9 Hz, 1H), 7.87 (dd, *J* = 8.1, 0.9 Hz, 1H), 7.65 (dd, *J* = 7.72, 1.1 Hz, 1H), 7.59–7.16 (m, 10H), 5.65 (dd, *J* = 10.1, 9.0 Hz, 1H), 5.25 (dd, *J* = 10.3, 9.0 Hz, 1H), 5.10 (dd, *J* = 7.0, 6.9 Hz, 1H), 4.72 (t, *J* = 8.0 Hz, 1H), 4.65–4.49 (m, 2H), 1.99 (s, 3H), 1.68 (s, 3H). ¹³C{¹H} NMR (CDCl₃, 22 °C, 75 MHz): δ 178.3, 171.3, 169.5, 168.2, 155.9, 141.8, 141.3, 141.14, 141.1, 137.7, 129.4, 129.3, 128.5, 128.3, 127.5,

127.2, 124.5, 80.0, 67.5, 65.6, 58.8, 22.8, 21.3. Anal. Calcd for C₂₇H₂₅N₃O₆Pd: C, 54.60 (54.56); H, 4.24 (3.46).

Acknowledgment. We acknowledge an EpSCOR grant to the University of Arkansas and the Arkansas Bioscience Institute for support of this research.

Supporting Information Available: Figures giving ¹H NMR spectra and tables giving crystal structure data for all new compounds; crystal data are also available as CIF files. This material is available free of charge via the Internet at <http://pubs.acs.org>.

OM050755K